

<https://doi.org/10.1038/s41531-024-00813-z>

Progression trajectories from prodromal to overt synucleinopathies: a longitudinal, multicentric brain [^{18}F]FDG-PET study

Check for updates

Beatrice Orso ¹✉, Pietro Mattioli^{1,2}, Eun-Jin Yoon ³, Yu Kyeong Kim⁴, Heejung Kim ⁴, Jung Hwan Shin ⁵, Ryul Kim ⁶, Francesco Fama^{1,2}, Andrea Brugnolo^{1,7}, Federico Massa^{1,8}, Agostino Chiaravalloti^{9,10}, Mariana Fernandes¹¹, Matteo Spanetta¹², Fabio Placidi^{11,13}, Matteo Pardini^{1,8}, Matteo Bauckneht ^{14,15}, Silvia Morbelli^{16,17}, Jee-Young Lee¹⁸, Claudio Liguori^{11,13} & Dario Arnaldi ^{1,2}

The phenoconversion trajectory from idiopathic/isolated Rapid eye movement (REM) sleep behavior disorder (iRBD) towards either Parkinson's Disease (PD) or Dementia with Lewy Bodies (DLB) is currently uncertain. We investigated the capability of baseline brain [^{18}F]FDG-PET in differentiating between iRBD patients eventually phenoconverting to PD or DLB, by deriving the denovoPDRBD-related pattern (denovoPDRBD-RP) from 32 de novo PD patients; and the denovoDLBRBD-RP from 30 de novo DLB patients, both with evidence of RBD at diagnosis. To explore [^{18}F]FDG-PET phenoconversion trajectories prediction power, we applied these two patterns on a group of 115 iRBD patients followed longitudinally. At follow-up (25.6 ± 17.2 months), 42 iRBD patients progressed through overt alpha-synucleinopathy (21 iRBD-PD and 21 iRBD-DLB converters), while 73 patients remained stable at the last follow-up visit (43.2 ± 27.6 months). At survival analysis, both patterns were significantly associated with the phenoconversion trajectories. Brain [^{18}F]FDG-PET is a promising biomarker to study progression trajectories in the alpha-synucleinopathy continuum.

Rapid eye movement (REM) sleep behavior disorder (RBD) is a specific manifestation of the prodromal stage of α -synucleinopathies. Indeed, during follow-up, the vast majority of individuals with isolated/idiopathic RBD (iRBD) eventually develop parkinsonism and/or dementia¹⁻⁴. However, given the heterogeneous nature of iRBD, the time of phenoconversion to a full-blown α -synucleinopathy is highly diverse, with some patients remaining "isolated/idiopathic" up to 10 years following diagnosis⁵⁻⁷. Nevertheless, this population is the ideal target for testing disease-modifying therapies, once available⁸.

The increasing interest in determine a biological definition of α -synucleinopathies is highlighting how Parkinson's disease (PD) and Dementia with Lewy bodies (DLB) actually belong to the same disease spectrum⁹.

However, PD and DLB have clear syndromic differences, and the overall prognosis is not necessarily the same. For example, DLB is associated with a worst quality of life, higher mortality rates, and caregiver burden¹⁰. Thus, it would be not only important to be able to predict whether iRBD patients would eventually phenoconvert on the short-term, but also whether they would develop a parkinsonism or dementia-first phenotype.

¹Department of Neuroscience, Rehabilitation, Ophthalmology, Genetics, Maternal and Child Health (DINO GMI), University of Genoa, Genoa, Italy. ²Neurophysiology Unit, IRCCS Ospedale Policlinico S. Martino, Genoa, Italy. ³Memory Network Medical Research Center, Seoul National University, Seoul, Republic of Korea. ⁴Department of Nuclear Medicine, Seoul National University College of Medicine and Seoul Metropolitan Government-Seoul National University Boramae Medical Center, Seoul, Republic of Korea. ⁵Department of Neurology, Seoul National University College of Medicine, Seoul, Republic of Korea. ⁶Department of Neurology, Inha University Hospital, Incheon, Republic of Korea. ⁷Clinical Psychology Unit, IRCCS Ospedale Policlinico S. Martino, Genoa, Italy. ⁸Clinical Neurology Unit, IRCCS Ospedale Policlinico S. Martino, Genoa, Italy. ⁹IRCCS Neuromed, Pozzilli, Italy. ¹⁰Department of Biomedicine and Prevention, University of Rome "Tor Vergata", Rome, Italy. ¹¹Department of Systems Medicine, University of Rome "Tor Vergata", Rome, Italy. ¹²Santa Maria della Stella Hospital, Orvieto, Italy. ¹³Sleep Medicine Center, Neurology Unit, University Hospital "Tor Vergata", Rome, Italy. ¹⁴Department of Health Science (DISSAL), University of Genoa, Genoa, Italy. ¹⁵Nuclear Medicine Unit, IRCCS Ospedale Policlinico S. Martino, Genoa, Italy. ¹⁶Nuclear Medicine Unit, AOU Città Della Salute e Della Scienza di Torino, Torino, Italy. ¹⁷Department of Medical Sciences, University of Turin, Turin, Italy. ¹⁸Department of Neurology, Seoul National University College of Medicine and Seoul Metropolitan Government-Seoul National University Boramae Medical Center, Seoul, Republic of Korea. ✉ e-mail: beatrice27orso@gmail.com

Over the past few years, researchers focused on the identification of biomarkers able to study disease progression and their association with phenoconversion in iRBD¹¹. Among these, brain [¹⁸F]FDG-PET has shown to be a valuable biomarker of neurodegeneration in both prodromal and overt stages of alpha-synucleinopathies, and longitudinal studies showed that brain [¹⁸F]FDG-PET is a reliable predictor of phenoconversion in iRBD patients^{12–14}. Several cross-sectional studies identified disease-specific patterns of alpha-synucleinopathies, such as PD^{15,16} and DLB^{16,17}, as well as a specific iRBD-related pattern (RBD-RP)^{13,18}; interestingly, these patterns showed a certain degree of spatial overlap. Although, the brain areas involved slightly change depending on the clinical syndromes. For example, in PD different brain glucose features are evident based on the presence/absence of cognitive impairment¹⁹, or the disease stage (i.e., de novo versus overt stage)²⁰.

This suggests that brain [¹⁸F]FDG-PET is able to capture the clinical and severity differences along the same pathological spectrum. Putting this concept into the prodromal stage's scenario, we hypothesized that brain [¹⁸F]FDG-PET may be able to identify not only iRBD patients at high risk of short-term phenoconversion, but also to be associated to the phenoconversion trajectory (i.e., parkinsonism-first versus dementia-first).

To test this, we hypothesized that the typical brain glucose patterns seen in patients with overt parkinsonism or dementia may be already present in the prodroma stage, i.e., in those iRBD patients that would develop parkinsonism or dementia, respectively, over time. To note, it has been demonstrated that the brain glucose pattern of iRBD patients changes approaching phenoconversion, showing, on the one hand, a reduction of its expression and, on the other, an increase of the PD-related pattern expression¹³. This finding suggests that iRBD patients closer to phenoconversion should have higher expression of the respective full-blown alpha-synucleinopathy patterns, compared with iRBD patients with a lower likelihood of short-term phenoconversion.

In this prospective longitudinal cohort study, we first studied brain [¹⁸F]FDG-PET of de novo PD patients with evidence of RBD (denovoPDRBD) and de novo DLB with evidence of RBD (denovoDLBRBD) and then identified the denovoPDRBD-related pattern (denovoPDRBD-RP) and the denovoDLBRBD-related pattern (denovoDLBRBD-RP). This choice is led by the idea that de novo patterns are likely to reflect the metabolic characteristics that iRBD patients would have at the time of phenoconversion to overt PD or DLB.

As a second step, we applied these patterns (denovoPDRBD-RP and denovoDLBRBD-RP) in a large group of iRBD patients longitudinally followed, to explore their capability in differentiating between iRBD-PD converters and iRBD-DLB converters (i.e., parkinsonism-first and dementia-first phenotypes respectively).

Results

Descriptive analysis

De novo PD and DLB patients were older and had lower education and lower MMSE when compared with HC (Supplementary Table 1). Moreover, iRBD non-converter patients were younger, had lower MDS-UPDRS-III scores, and were also less classified as MCI, when compared with iRBD-converter patients (Table 1). A higher number of iRBD-DLB converters were also classified as MCI compared to iRBD-PD converters (Table 2).

When comparing center-specific characteristics, a significant difference in MDS-UPDRS-III scores in both iRBD-converters and non-converters ($p < 0.001$), with lower scores in the Italian centers, was found; moreover, iRBD non-converters Seoul patients had a lower MMSE, a longer follow-up time and a fewer number of males enrolled compared to Genoa and Rome Tor Vergata patients (Supplementary Table 2). There were no significant differences in iRBD-PD converters across centers ($p = 0.445$); while Seoul iRBD-DLB converters had a higher MDS-UPDRS-III scores compared to Genoa and Rome Tor Vergata iRBD-DLB converters (Supplementary Table 2).

Table 1 | Demographic and clinical characteristics of iRBD patients

	iRBD-converters patients <i>n</i> = 42	iRBD non-converters patients <i>n</i> = 73	<i>p</i> -value
Age, years	72.23 ± 5.45; 72 [61–84]	68.9 ± 6; 69 [56–82]	0.005
Education, years	10 ± 4.5; 8 [2–18]	9.9 ± 4.37; 8 [0–18]	0.91
Sex, males	31 (73.8%)	50 (68.5%)	0.547
MMSE	27.45 ± 2.24; 28 [22–30]	28.08 ± 1.9; 29 [23–30]	0.12
MDS-UPDRS-III	4.35 ± 4.53; 3.5 [0–17]	2.76 ± 3.64; 1 [0–18.5]	0.04
MCI (Y:N)	28:14	28:45	0.003
Phenoconversion			
Survival Time (months)	25.59 ± 17.17; 23 [3–84]	43.2 ± 27.64; 30 [7–137]	0.0006
PD	21 (50%)	/	
DLB	21 (50%)	/	
MSA	0	/	

Continuous variables are shown as mean ± standard deviation; median [range]. Categorical variables are shown as number (percentage). Significant *p*-values are reported in bold. DLB Dementia with Lewy bodies, MCI mild cognitive impairment, MDS-UPDRS-III Movement Disorders Society-sponsored revision of the Unified Parkinson's Disease Rating Scale, motor section, MMSE Mini-Mental State Examination, PD Parkinson's Disease, iRBD idiopathic REM sleep behaviour disorder, REM Rapid eyes movements.

Table 2 | Demographic and clinical characteristics of iRBD-converters patients

	iRBD-PD converters patients <i>n</i> = 21	iRBD-DLB converters patients <i>n</i> = 21	<i>p</i> -value
Age, years	71 ± 5.52; 72 [61–79]	73 ± 5.23; 72 [66–83]	0.235
Education, years	10 ± 4.6; 8 [2–17]	10 ± 4.6; 8 [5–18]	1
Sex, males	14 (70%)	17 (77.2%)	0.726
MMSE	28 ± 2; 28 [23–30]	27 ± 2.4; 28 [24–30]	0.15
MDS-UPDRS-III	5 ± 4.56; 4 [0–17]	4 ± 4.4; 2 [0–17]	0.473
MCI (Y:N)	11:10	17:4	0.53
Survival Time (months)	29 ± 18.3; 30 [3–84]	22 ± 15.7; 18 [3–60]	0.19

Continuous variables are shown as mean ± standard deviation; median [range]. Categorical variables are shown as number (percentage). DLB Dementia with Lewy bodies, MCI Mild Cognitive Impairment, MDS-UPDRS-III Movement Disorders Society-sponsored revision of the Unified Parkinson's Disease Rating Scale, motor section, MMSE Mini-Mental State Examination, PD Parkinson's Disease, iRBD idiopathic REM sleep behaviour disorder, REM Rapid eyes movements.

denovoPDRBD and denovoDLBRBD-related patterns

For the denovoPDRBD-RP, PCs 1 and 2 were the one that best discriminated between patients and controls, with a cumulative variance of 59%, while the denovoDLBRBD-RP was built on a combination of PCs 1 and 2, which explained the 58.9% of the variance.

Thresholded voxels after bootstrap resembling (2.5%–97.5% CI) were overlaid on a T1-MRI template for visualization (Fig. 1A, B) and then topographically overlapped (Fig. 1C).

Both the denovoPDRBD-RP and the denovoDLBRBD-RP showed the presence of positive voxel weights in the frontal regions, putamen/pallidus, thalamus, brainstem, pons, and the anterior cingulate cortex, while negative components were found in parietal and occipital areas (Fig. 1A, B). When

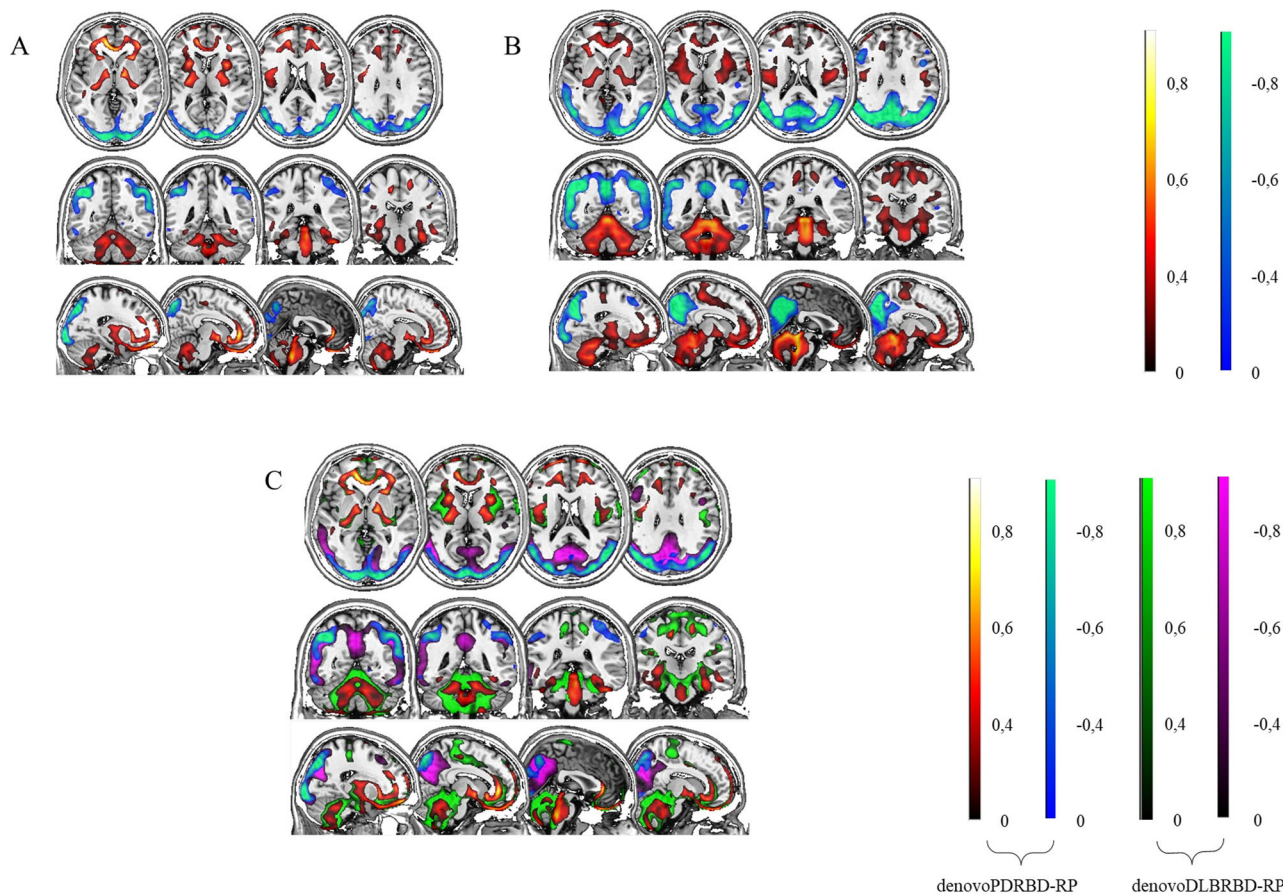


Fig. 1 | Results of the SSM-PCA. A Display of stable voxels of the denovoPDRBD-RP. Red indicates positive voxel weights (relative hypermetabolism) in denovoPDRBD-RP, while Blue indicates negative voxel weights (relative hypometabolism) in denovoPDRBD-RP. B Display of stable voxels of the denovoDLBRBD-RP. Red indicates positive voxel weights (relative hypermetabolism) in denovoDLBRBD-RP, while Blue indicates negative voxel weights (relative

hypometabolism) in denovoDLBRBD-RP. C Overlapping of the denovoPDRBD-RP and denovoDLBRBD-RP. Red indicates positive voxel weights (relative hypermetabolism) in denovoPDRBD-RP, while Blue indicates negative voxel weights (relative hypometabolism) in denovoPDRBD-RP. Green indicates positive voxel weights (relative hypermetabolism) in denovoDLBRBD-RP, while Pink indicates negative voxel weights (relative hypometabolism) in denovoDLBRBD-RP.

overlayed, the denovoDLBRBD-RP showed a wider area of negative components, extending to the precuneus, compared to the denovoPDRBD-RP, as well as a greater involvement of positive components in the cerebellum and vermis (Fig. 1C).

Given the high rate of overlap, the two patterns were significantly correlated between each other ($p < 0.001$).

Phenoconversion prediction ability of the denovoPDRBD-RP

The ANOVA showed a significant difference ($p = 0.003$) between the pattern expression of iRBD non-converters and iRBD-converters (either to PD or DLB). In detail, the post-hoc analysis showed a significant difference between iRBD non-converters and iRBD-PD converters ($p = 0.042$) and iRBD-DLB converters ($p = 0.011$), respectively, while there was no difference between iRBD-PD converters and iRBD-DLB converters ($p = 0.947$) (Fig. 2A). At ROC analysis the denovoPDRBD-RP was able to discriminate between iRBD-PD converters and iRBD-DLB converters with 73% sensitivity and 50% specificity (AUC = 0.61), with a negative predicting value (NPV) of 0.38 and a positive PV (PPV) of 0.64. Time-dependent ROC analyses for the denovoPDRBD-RP expression revealed an increase in AUC after one year, with a steady decline from month 24 (month 12: AUC 0.71; month 24: AUC 0.70; month 36: AUC 0.68; month 48: AUC 0.60; month 60: AUC 0.59; month 72: AUC 0.59; month 84: AUC 0.59). No significant correlation was found between the denovoPDRBD-RP expression and MMSE ($p = 0.346$), while pattern expression negatively correlated with survival time ($p = 0.021$) and positively with the MDS-UPDRS-III score ($p = 0.012$).

Kaplan–Meier curves are reported in Fig. 2B, the empirical optimal cut-off chosen as threshold is 1.075. The prediction model was statistically significant ($p = 0.007$). On Cox regression analysis, iRBD who expressed the denovoPDRBD-RP over 1.075 had a significantly high risk of phenoconverting to DLB instead of PD (age and center adjusted HR of 3.21, $p = 0.029$, C.I.95%: 1.12–9.18).

Phenoconversion prediction ability of the denovoDLBRBD-RP

The ANOVA showed a significant difference ($p = 0.001$) between the pattern expression of iRBD non-converters and iRBD-converters (either to PD or DLB). At post-hoc analysis, a significant difference between iRBD non-converters and iRBD-PD converters ($p = 0.040$) and iRBD-DLB converters ($p = 0.002$) respectively, while there was no difference between iRBD-PD converters and iRBD-DLB converters ($p = 0.718$) (Fig. 3A). At ROC analysis the denovoDLBRBD-RP was able to discriminate between iRBD-DLB converters and iRBD-PD converters with 77% sensitivity and 55% specificity (AUC = 0.66), with a NPV of 0.68 and a PPV of 0.65. Time-dependent ROC analyses for the denovoDLBRBD-RP expression showed that the AUC remained stable throughout follow-up time, with an increase of the AUC in the third year (month 12: AUC 0.62; month 24: AUC 0.64; month 36: AUC 0.74; month 48: AUC 0.69; month 60: AUC 0.66; month 72: AUC 0.66; month 84: AUC 0.66). No significant correlation was found between the denovoDLBRBD-RP expression and MMSE ($p = 0.191$), while pattern expression negatively correlated with survival time ($p = 0.034$) and positively with the MDS-UPDRS-III score ($p = 0.023$).

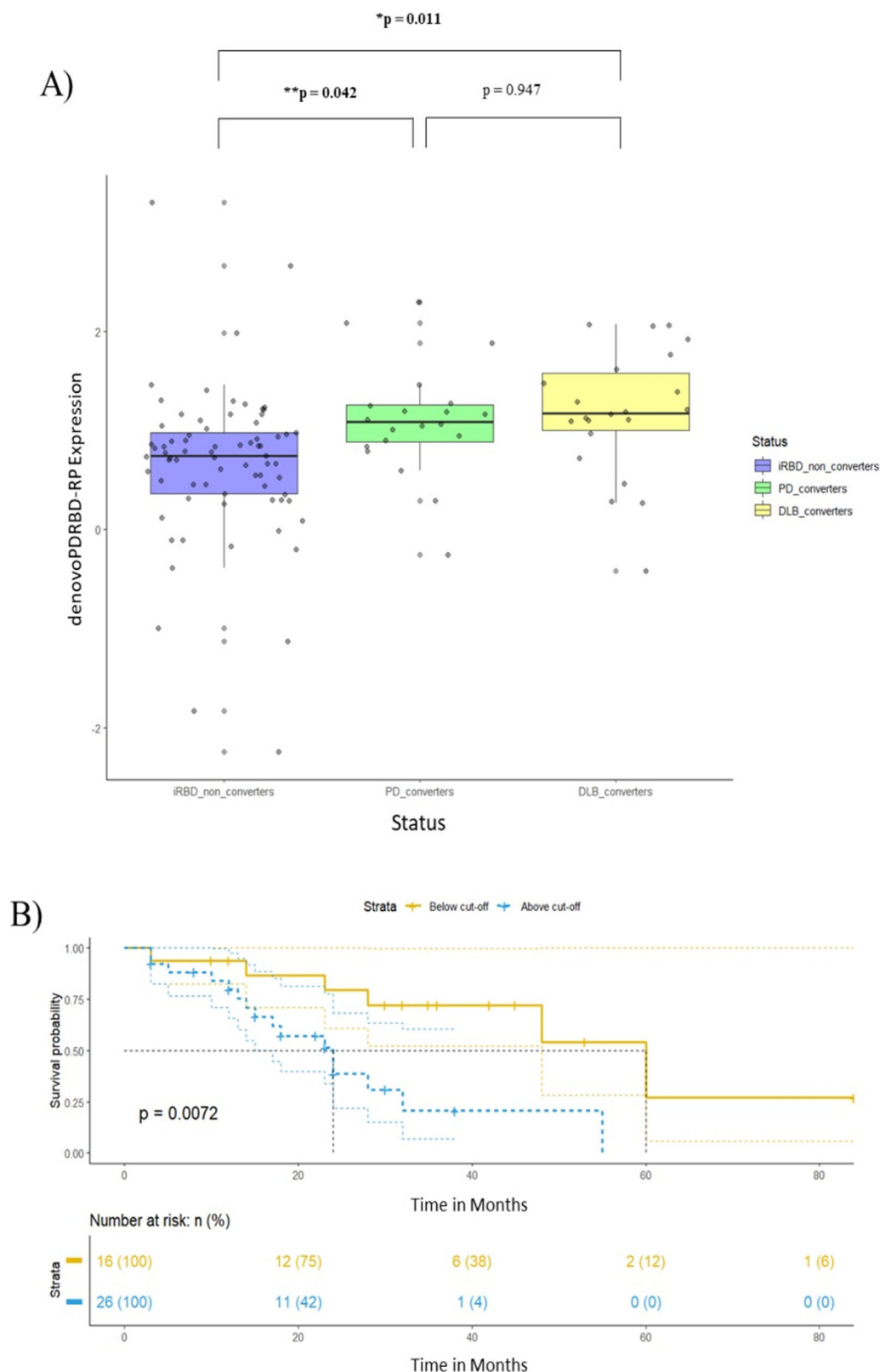


Fig. 2 | Results of the ANOVA and survival analysis in the denovoPDRBD-RP. **A** Distribution of subject's z-scores in iRBD groups, with the optimum discrimination threshold (empirical cut-point = 1.075). (Purple = iRBD non-converters; Green = iRBD-PD converters; Yellow = iRBD-DLB converters) **B** Results of

the Survival analysis of the denovoPDRBD-RP expression on iRBD-PD and iRBD-DLB converters. Blue line = denovoPDRBD-RP expression below the empirical optimal cut-point. Orange line = denovoPDRBD-RP expression above the empirical optimal cut-point.

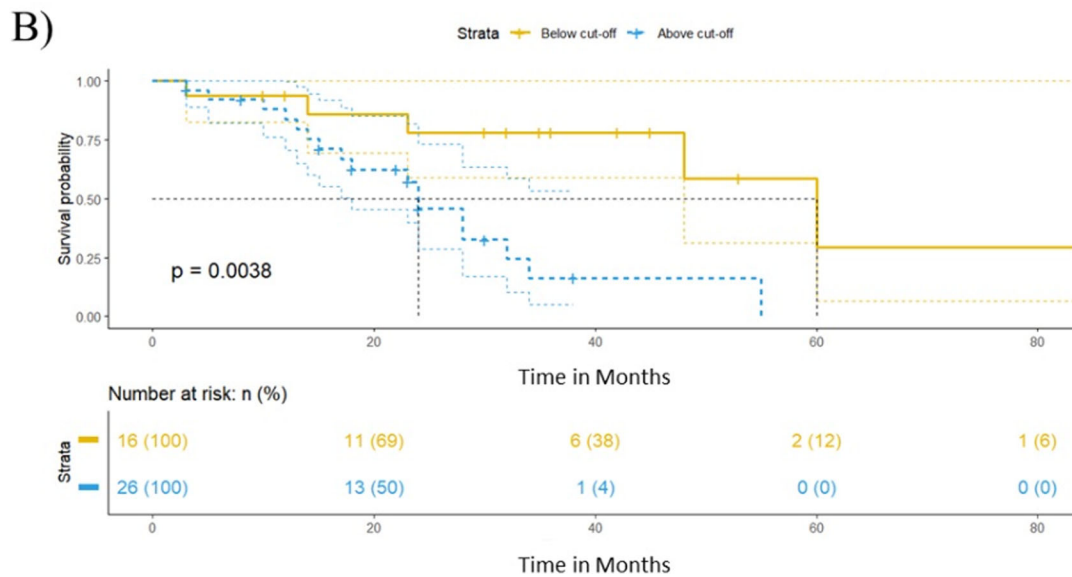
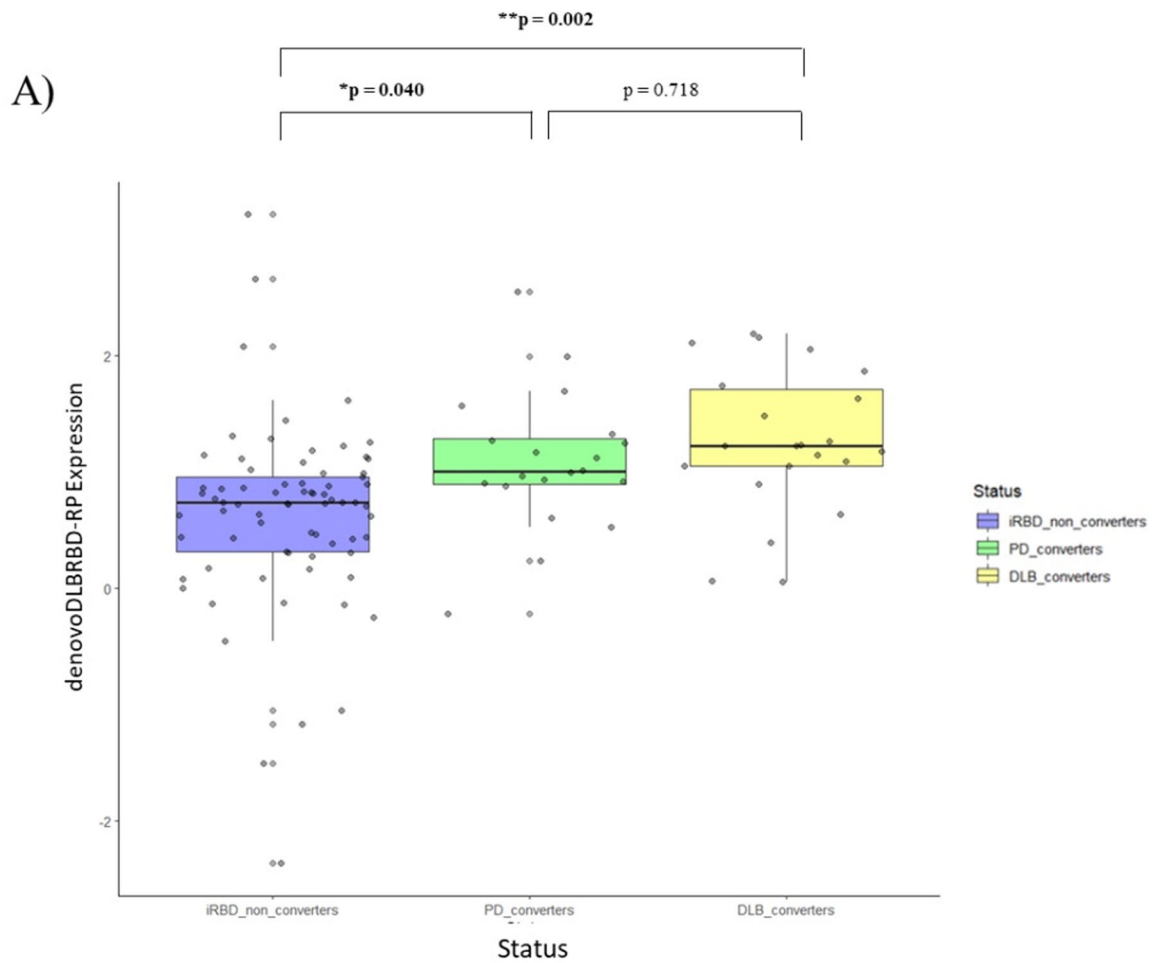


Fig. 3 | Results of the ANOVA and Survival Analysis in the denovoDLBRBD-RP.

A Distribution of subject's z-scores in iRBD groups, with the optimum discrimination threshold (empirical cut-point = 1.028). (Purple = iRBD non-converters; Green = iRBD-PD converters; Yellow = iRBD-DLB converters) B Results of

the Survival analysis of the denovoDLBRBD-RP expression on iRBD-PD and iRBD-DLB converters. Blue line = denovoDLBRBD-RP expression below the empirical optimal cut-point. Orange line = denovoDLBRBD-RP expression above the empirical optimal cut-point.

Kaplan–Meier curves are reported in Fig. 3B, the empirical optimal cut-off chosen as threshold is 1.028. The prediction model was statistically significant ($p = 0.003$). On Cox regression analysis, iRBD patients expressing the denovoDLBRBD-RP over 1.028 had a high risk of phenoconverting to DLB instead of PD (age and center adjusted HR of 3.52, $p = 0.034$, C.I.95%: 1.09–11.27).

All the aforementioned analyses (both on the denovoPDRBD-RP and the denovoDLBRBD-RP) were also performed after applying the ComBat harmonization toolbox^{21,22} on the subject scores representing the pattern expression, to correct for site variability (i.e., scanner-to-scanner variability, while preserving biological associations). Results did not substantially change, although the significance of the models was slightly lower.

Furthermore, when qualitatively investigating both patterns expression, we found that 25 of the 42 iRBD phenoconverted patients express both patterns, 64% being iRBD–DLB phenoconverted patients.

Among the 42 iRBD phenoconverted patients, one expressed only the denovoPDRBD-RP at baseline (and it was an iRBD–PD phenoconverted subject at follow-up), one expressed only the denovoDLBRBD-RP at baseline (and it was an iRBD–DLB phenoconverted subject at follow-up), and 15 patients did not express either pattern, 60% being iRBD–PD phenoconverted patients.

Clinical features

As expected, there was a significant difference between iRBD non-converters and iRBD-converters (both iRBD–PD and iRBD–DLB converters) regarding the presence of baseline MCI ($p = 0.003$). However, no significant difference was found between iRBD–PD and iRBD–DLB converters ($p = 0.53$). Indeed, the presence of MCI showed a sensitivity of 36%, specificity of 53%, and an accuracy of 38% in discriminating between iRBD–PD and iRBD–DLB converters. Finally, the presence of MCI at baseline was not significantly associated with the phenoconversion trajectory ($p = 0.322$, adjusted HR 1.59, C.I.95%: 0.63–3.98).

Considering these results, we performed a further analysis aimed at investigating whether the presence of MCI combined with pattern expression characteristics could better discriminate between phenoconversion trajectories. We choose to use the denovoDLBRBD-RP because of the slightly higher adjusted HR at Cox regression analysis; hence we applied the aforementioned empirical optimal cut-off of 1.028 to identify patients at higher risk of developing a dementia-first phenotype. Therefore, we divided the 42 iRBD-converters patients into 4 groups, as follows: phenoconverted patients with MCI at baseline and above the empirical optimal cut-off ($n = 17$, PD converters = 6, DLB converters = 11); phenoconverted patients without MCI at baseline and below the empirical optimal cut-off ($n = 7$, PD converters = 5, DLB converters = 2); phenoconverted patients without MCI at baseline and above the empirical optimal cut-off ($n = 9$, PD converters = 3, DLB converters = 6); phenoconverted patients with MCI at baseline and below the empirical optimal cut-off ($n = 9$, PD converters = 6, DLB converters = 3). No significant difference was found amongst the four groups ($p = 0.197$). It is interesting to notice that, in the group of patients without MCI at baseline but above the empirical optimal cut-off, the majority phenoconverted to DLB, which could be unexpected.

Overall, these results suggest that patients with a higher expression of the denovoDLBRBD-RP have a high likelihood of developing DLB regardless the baseline MCI status.

Finally, we also explore Cox regression models on the expression of both patterns, separately, adjusting for age, center, MDS–UPDRS–III, and MMSE scores. When including MDS–UPDRS–III and MMSE to the model, iRBD patients who expressed the denovoPDRBD-RP over 1.075 had a significantly high risk of phenoconverting to DLB instead of PD (HR of 5.44, $p = 0.006$, C.I.95%: 1.59–18.59), while iRBD patients who expressed the denovoDLBRBD-RP over 1.028 had a significantly high risk of phenoconverting to DLB instead of PD (HR of 7.58, $p = 0.003$, C.I.95%: 1.78–32.19).

Discussion

In the present study, we identified two different brain metabolic patterns able to discriminate iRBD phenoconversion trajectories, either PD or DLB. Our a priori hypothesis was that disease-specific related patterns (i.e., PD-related and DLB-related) would have been able to identify PD converters and DLB converters, respectively. Instead, we found that baseline high expression of both the denovoPDRBD-RP and denovoDLBRBD-RP significantly identified iRBD–DLB over iRBD–PD converters with similar performances, even if the denovoDLBRBD-RP showed slightly higher AUC and hazard ratio values. This finding may be counterintuitive, since it may be expected that patients with a high denovoPDRBD-RP expression would develop a parkinsonism-first phenotype, instead of the dementia-first one. The reason of this finding may be explained looking in details at the characteristics of the two overt stages brain glucose patterns.

As a matter of fact, despite an expected partial overlap, the denovoDLBRBD-RP appears to express a more severe and wider metabolic pattern, with the extension of the impairment to the precuneus and the cerebellum, compared with the denovoPDRBD-RP. The spatial covariance analysis applied to identify the patterns allows to highlight voxels that either positively or negatively covary together, thus, from a clinical standpoint we could speculate that the positive and negative components represent relatively higher and lower metabolism, respectively. With this being said, both the denovoPDRBD-RP and the denovoDLBRBD-RP showed the presence of positive voxel weights in the putamen/pallidus, thalamus, pons, and the anterior cingulate cortex, while negative components were found in parietal and occipital areas, with a more pronounced metabolic decrease in the precuneus in the denovoDLBRBD-RP. This evidence is not only in line with the more widespread involvement of the cortex in DLB compared to PD patients but, more interestingly, it points out how these two patterns are placed on the same pathological continuum. Specifically, denovoDLBRBD-RP seems to represent a more severe expression of the Lewy body disorders continuum.

From a clinical standpoint, DLB patients usually show signs and symptoms negatively impacting the quality of life, since the earlier phases of the disease¹⁰. Conversely, de novo PD patients may preserve most of their social and working functioning, showing a limited impact on their quality of life in the early stages of the disease. This may reflect a higher burden of disease in de novo DLB patients compared with de novo PD patients. Thus, it may be speculated, that iRBD developing a dementia-first phenotype may have a more aggressive disease, likely paralleled by a more severe neurodegeneration, compared with iRBD patients developing a parkinsonism-first phenotype. This is in line with a recent multicentric study showing how iRBD patients developing a dementia-first phenotype had more severe baseline neurodegeneration of the dopaminergic nigro-striatal system²³. Following this concept, it is not surprising that iRBD patients showing more impaired brain glucose metabolism (i.e. higher expression of either denovoPDRBD-RP or the denovoDLBRBD-RP) develop a dementia-first phenotype. Indeed, brain [¹⁸F]FDG-PET, as a well-known biomarker of neurodegeneration, has been suggested to be used for staging neurodegeneration, in the recent proposal for a new staging system in PD²⁴.

Interestingly, in our study, both patterns were significantly correlated with motor but not cognitive scores. This supports the concept that the MDS–UPDRS–III is a better disease marker than MMSE in alpha-synucleinopathies. Indeed, despite it is widely used both in clinical and research settings, MMSE has several limitations, especially in alpha-synucleinopathies, possibly related to floor or roof effects²⁵.

Over the last decade, researchers have been focusing on the identification of robust, reliable, and replicable biomarkers able to mark disease progression and predict the type of phenoconversion at baseline. Although, this is not an easy task, given the high heterogeneity in the time of phenoconversion, symptoms manifestation, and the well-known similarities between de novo PD with RBD and de novo DLB with RBD. In literature, clinical data have shown only moderate ability in predicting the outcome diagnosis, with the most promising marker being the presence of MCI¹. However, in the present study, we showed that the presence of MCI at

baseline, both alone and combined with brain glucose characteristics, was not significantly associated with phenoconversion over time. On the other hand, it has been shown that combination of MCI and the presence of linguistic abnormalities might provide a predictor of phenoconversion from iRBD to dementia-first phenotype²⁶. Moreover, we showed that when combining neuroimaging with clinical data, such as MDS-UPDRS-III and MMSE, the association with phenoconversion from iRBD to dementia-first phenotype is stronger, compared to neuroimaging or neuroimaging and MCI alone.

Within this scenario, [¹⁸F]FDG-PET may be a good biomarker of both phenoconversion and clinical outcome. Indeed, it has been already demonstrated that brain [¹⁸F]FDG-PET, assessed with spatial covariance analysis^{18,27}, is a strong biomarker of phenoconversion. However, iRBD patients may phenoconvert to PD, DLB, and a minority of them to multiple system atrophy. Therefore, to enlarge the prediction power ability of the brain [¹⁸F]FDG-PET, we recently identified a pattern of brain glucose metabolism associated with phenoconversion in iRBD (iRBDconvRP), regardless the final diagnosis¹². This pattern showed to be a robust and reliable biomarker for identifying iRBD phenoconverters, and it was subsequently replicated in an independent cohort of patients, confirming its reliability^{12,28}.

In summary, our data suggest that having an increased expression of the overt PD/DLB-related patterns, especially the denovoDLBRBD-RP, already in the iRBD stage, may be considered as a predictor of the “dementia-first” phenotype, with a probability of 68% and a hazard ratio of 3.52, while patterns’ lower expression in the prodromal phase as a predictor of the “parkinsonism-first” syndrome. To note, both patterns were significantly correlated with survival time, confirming previous longitudinal data suggesting that brain [¹⁸F]FDG-PET may be a candidate surrogate disease progression biomarker^{13,15}. This result should be combined with the notion that iRBD patients with a more severe baseline brain glucose metabolism pattern are at high risk of short-term phenoconversion^{12,13,20}.

From a practical point of view, these findings suggest that neurodegeneration biomarkers, especially brain [¹⁸F]FDG-PET, may show different levels of abnormalities, likely related with different prognosis. That is, iRBD patients with normal brain [¹⁸F]FDG-PET might have a lower risk of phenoconversion on the short-term, iRBD patients with mild to moderate brain glucose metabolism impairment have a high risk of short-term phenoconversion, likely a parkinsonism-first phenotype, while iRBD patients showing a severe brain glucose metabolism impairment might have a high risk of developing a dementia-first phenotype at short-term. The optimal cut-points to identify those neurodegeneration levels need to be identified in larger longitudinal studies. This may be relevant in a clinical trial setting, in which using the same biomarker (i.e., brain [¹⁸F]FDG-PET), it may be feasible to both apply a phenoconversion pattern (i.e., the iRBDconvRP) to select patients to be enrolled, and to stratify them using a trajectory pattern (i.e., the denovoDLBRBD-RP) for secondary analyses.

This study has some limitations and strengths. Firstly, while the link between brain glucose metabolism and iRBD phenoconversion seems promising, several challenges need to be addressed, such as the need for larger longitudinal studies, and multi-center collaborations to confirm and validate the present results, always taking into account the standardization of imaging protocols. In this light, the present study is multicentric and includes patients with different ethnicities (i.e., Caucasian and Asian). However, it must be highlighted that both the denovoDLBRBD-RP and the denovoDLBRBD-RP were derived in a Caucasian cohort of patients, and they were subsequently applied also on an Asian cohort of patients. On one hand, this may have contributed to lowering the prediction ability of the patterns. On the other hand, the results found in the present study, suggest that those measurements might be broadly applicable. Addressing this issue will be of utmost importance for future clinical trials. Secondly, the [¹⁸F]FDG-PET protocol used in the three centers was not a-priori harmonized. Notably, after harmonizing the data by correcting for site variability the results did not change, thus suggesting the solidity of the data. Moreover, given the rising importance on the biological definition of Lewy body

disorders, not every patient enrolled in this study had neuronal synuclein diseases defined biologically on the basis of an in-vivo biomarker, namely CSF or skin biopsy⁹. Lastly, a more in-depth view of the relationship between cognitive performance and the brain metabolic pattern expressed by these patients might help in differentiating the phenoconversion trajectories. Although often the neuropsychological batteries used across centers are not harmonized this issue highlights the need of joined effort from different centers specialized in iRBD to provide soon a harmonized neuropsychological battery, so to increase quality in the sharing process and data analysis.

Methods

Patients

From the Genoa center, we enrolled 32 de novo PD patients (mean age: 73.12 ± 5.86 y.o; 22 males) and 30 de novo DLB patients (mean age 78 ± 4.4 y.o, 18 males) with evidence of RBD, as well as 44 Healthy Controls (HC, mean age: 69 ± 6 y.o; 16 males). Diagnosis was performed following current criteria^{29,30} and confirmed by the evidence of presynaptic dopaminergic deficit on [¹²³I]FP-CIT SPECT and by at least two years of follow-up. Diagnosis of RBD was confirmed by video-polysomnography (vPSG), according to current criteria³¹, in all PD patients and in thirteen DLB patients (43.3%). In the remaining seventeen DLB patients, a suggestive and persistent clinical history of RBD presence was reported. Brain MRI or CT was used to rule out brain diseases^{32,33}. The presence of white matter hyperintensities was not an exclusion criterion if the Wahlund scale was not >1 for each brain region³⁴. At baseline, all patients underwent the Movement Disorder Society Unified Parkinson Disease rating scale, the third part (MDS-UPDRS-III) to quantify motor impairment, the Mini-Mental State Examination (MMSE), as a measure of global cognitive functioning, as well as a comprehensive neuropsychological assessment of the main cognitive domains (verbal memory, executive functions, attention, and working memory, visuospatial abilities and language)³². Presence of mild cognitive impairment (MCI) was defined as the significant decline on at least two tests, either within a single cognitive domain or across different cognitive domains³⁵.

Furthermore, from two Italian centers, Genoa and Rome Tor Vergata, and a South-Korean one (Seoul) we enrolled 115 iRBD patients, of whom 42 iRBD patients (mean age: 72.2 ± 5.4, 31 males, follow-up time: 25 ± 17 months) subsequently phenoconverting to an overt alpha-synucleinopathy (iRBD-converters, 21 PD and 21 DLB), and 73 iRBD patients (mean age: 68.9 ± 6 y.o, 50 males, follow-up time: 43 ± 27 months) not showing phenoconversion at follow-up (iRBD non-converters). To note, follow-up time refers to survival time, and it indicates the interval, expressed in months, between the date of [¹⁸F]FDG-PET acquisition and either phenoconversion date in converter patients, or the last follow-up visit in non-converter patients.

Diagnosis of RBD was confirmed by vPSG, according to current criteria³¹.

All iRBD patients underwent the same neurological and neuropsychological workup described above, following center-specific assessment^{32,33,36}. To note, the diagnosis of MCI was carried out following the same diagnostic criteria across each center³⁵.

Phenoconversion to overt alpha-synucleinopathy (i.e., PD, DLB, or MSA) was assessed using current diagnostic criteria for each neurodegenerative disorder^{29,30,37}.

[¹⁸F]FDG-PET and video-polysomnographic recording

All patients underwent [¹⁸F]FDG-PET to investigate brain glucose metabolism within 12 months from diagnosis, in accordance with the guidelines of the European Association of Nuclear Medicine in use at the time of acquisition^{38,39}.

Sleep scoring was performed following the current criteria⁴⁰. PSG derivations were placed according to recommended rules⁴⁰ to evaluate sleep features, respiratory, cardiac, and limb events. Patients were asked to withdraw melatonin, hypnotic medications, and antidepressant drugs for two weeks before the recording.

Center-specific acquisition and reconstruction protocols are described in detail elsewhere^{12,13,33,41}.

denovoPDRBD-RP and denovoDLBRBD-RP derivation and application

From the 32 de novo PD and 30 de novo DLB patients, both with evidence of RBD, along with 44 HC in the same age range, we derived the denovoPDRBD-RP and a denovoDLBRBD-RP by applying an automated algorithm, based on the SSM-PCA method⁴² implemented in Matlab (version 2020a; MathWorks, Natick, MA), to their [¹⁸F]FDG-PET data. Briefly, SSM-PCA was firstly applied on the [¹⁸F]FDG-PET images of 32 de novo PD patients and 44 HC. The resulting denovoPDRBD-RP was applied to the scans of 115 RBD patients (both converters and non-converters). The same analysis was performed on the [¹⁸F]FDG-PET images of 30 de novo DLB patients and 44 HC, to derive and apply the denovoDLBRBD-RP. For each subject, a score was calculated on each selected principal component (PC). The components that could best discriminate between controls and patients were linearly combined to form the disease-related pattern⁴³. The identification method is described in detail elsewhere^{12,44}.

For validation, we performed a leave-one-out cross-validation (LOOCV)¹², and to enhance the stability of the results, we performed a bootstrap resampling (1000 repetitions) to extract the most stable regions in the patterns obtained.

Standard protocol approval

All patients provided written informed consent before the enrolment in this study, in compliance with the Helsinki Declaration of 1975.

Study overview and statistical analysis

Once we derived the denovoPDRBD-RP and the denovoDLBRBD-RP, both patterns' expression was then computed, separately, on the [¹⁸F]FDG-PET scans of the 115 iRBD (both converters and non-converters) from Genoa, Rome Tor Vergata and Seoul. Subject scores of the iRBD-converters and non-converters patients, representing respectively the denovoPDRBD-RP and the denovoDLBRBD-RP expression, were z-transformed with respect to the corresponding center's HC group (the aforementioned 44 HC from Genoa, 11 HC from Rome Tor Vergata -mean age: 71 ± 3 y.o.; 6 males- and 24 HC from Seoul -mean age: 69 ± 5 y.o.; 7 males-).

Between-group differences in clinical characteristics were compared using unpaired t-test (normally distributed) or the Wilcoxon-Mann-Whitney test (non-normally distributed). Categorical variables were compared using χ^2 or Fisher's exact tests. Normal distribution of variables was checked using Shapiro-Wilk test.

A one-way analysis of variance (ANOVA) was performed on z-transformed subject scores to test patterns' ability to discriminate among groups, followed by Tukey-Kramer post hoc for pairwise-multiple comparison.

To determine the sensitivity and specificity of the patterns, a receiver operating curve (ROC) was plotted based on z-transformed subject scores from both patterns. The cut-off that gave optimum sensitivity and specificity, calculated with the Youden Index method⁴⁵, was chosen as the threshold. Moreover, time-dependent ROC curves were performed for each pattern and the Area Under the Curves (AUC) of each timepoint was compared (one-timepoint every twelve months, until month number 84).

Then, Kaplan-Meier survival analyses were performed to estimate the risk of phenoconversion from iRBD to either PD or DLB (in our sample, none of the iRBD converted to MSA) using the two separate patterns expression values (represented by the subject scores obtained), categorized as below or above the threshold previously computed by the Youden Index method. The survival time was set as the interval (expressed in months) between the date of [¹⁸F]FDG-PET acquisition and the date of phenoconversion in iRBD-converter patients.

In detail, the survival analyses were first performed using the subject scores obtained by applying the denovoPDRBD-RP on all iRBD-converters patients, then, the same analysis was run using the subject scores obtained by

applying the denovoDLBRBD-RP on the same cohort of iRBD-converters. In both cases, the two possible outcomes were the phenoconversion to PD and the phenoconversion to DLB, and the phenoconversion to DLB was arbitrary set as the failure event for computing the model. The adjusted hazard ratio (aHR) was calculated with a Cox regression, using age and center as covariates.

Partial Pearson's correlation analysis was performed between denovoPDRBD-RP and denovoDLBRBD-RP expression, separately, and (i) survival time, (ii) MDS-UPDRS-III score, (iii) MMSE score, and (iv) between one another, using age and center as a nuisance variable.

For comparison, we finally investigated differences in the presence of MCI amongst iRBD-PD and iRBD-DLB converters with Fisher's exact test and, using a Cox regression analysis, we saw whether the presence of MCI was associated with the risk of phenoconversion.

Statistical threshold was set at .05 and *p*-values were reported corrected for multiple comparisons using the Bonferroni approach.

All analyses were performed using MatLab (version 2020a; MathWorks, Natick, MA), Stata software (StataCorp. 2013. Stata Statistical Software: Release 13. College Station, TX: StataCorp LP) and R (R Core Team, 2020)-RStudio (Rstudio Team, 2020).

Data availability

The datasets used and/or analyzed during the current study available from the corresponding author on reasonable request.

Received: 1 July 2024; Accepted: 2 October 2024;

Published online: 25 October 2024

References

- Postuma, R. B. et al. Risk and predictors of dementia and parkinsonism in idiopathic REM sleep behaviour disorder: a multicentre study. *Brain* **142**, 744–759 (2019).
- Arnaldi, D. et al. Dopaminergic imaging and clinical predictors for phenoconversion of REM sleep behaviour disorder. *Brain* **144**, 278–287 (2021).
- Zhang, H. et al. Risk factors for phenoconversion in REM sleep behavior disorder. *Ann. Neurol.* **91**, 404–416 (2022).
- Galbiati, A., Verga, L., Giora, E., Zucconi, M. & Ferini-Strambi, L. The risk of neurodegeneration in REM sleep behavior disorder: a systematic review and meta-analysis of longitudinal studies. *Sleep Med. Rev.* **43**, 37–46 (2019).
- Iranzo, A. et al. Characterization of patients with longstanding idiopathic REM sleep behavior disorder. *Neurology* **89**, 242–248 (2017).
- Yao, C. et al. Longstanding disease-free survival in idiopathic REM sleep behavior disorder: is neurodegeneration inevitable? *Parkinsonism Relat. Disord.* **54**, 99–102 (2018).
- Arnaldi, D. et al. Brain glucose metabolism heterogeneity in idiopathic REM sleep behavior disorder and in Parkinson's disease. *J. Parkinsons Dis.* **9**, 229–239 (2019).
- Arnaldi, D. et al. Rapid eye movement sleep behavior disorder: a proof-of-concept neuroprotection study for prodromal synucleinopathies. *Eur. J. Neurol.* **28**, 1210–1217 (2021).
- Simuni, T. et al. A biological definition of neuronal α -synuclein disease: towards an integrated staging system for research. *Lancet Neurol.* **23**, 178–190 (2024).
- Chin, K. S., Teodorczuk, A. & Watson, R. Dementia with Lewy bodies: challenges in the diagnosis and management. *Aust. N. Z. J. Psychiatry* **53**, 291–303 (2019).
- Migliis, M. G. et al. Biomarkers of conversion to α -synucleinopathy in isolated rapid-eye-movement sleep behaviour disorder. *Lancet Neurol.* **20**, 671–684 (2021).
- Mattioli, P. et al. Derivation and validation of a phenoconversion-related pattern in idiopathic rapid eye movement behavior disorder. *Mov. Disord.* **38**, 7–67 (2022).

13. Kim, R. et al. Longitudinal changes in isolated rapid eye movement sleep behavior disorder-related metabolic pattern expression. *Mov. Disord.* **36**, 1889–1898 (2021).
14. Kogan, R. V. et al. Four-year follow-up of [18F] Fluorodeoxyglucose positron emission tomography-based Parkinson's disease-related pattern expression in 20 patients with isolated rapid eye movement sleep behavior disorder shows prodromal progression. *Mov. Disord.* **36**, 230–235 (2021).
15. Schindlbeck, K. A. & Eidelberg, D. Network imaging biomarkers: insights and clinical applications in Parkinson's disease. *Lancet Neurol.* **17**, 629–640 (2018).
16. Carli, G. et al. Comparison of univariate and multivariate analyses for brain [18F] FDG PET data in α -synucleinopathies. *NeuroImage Clin.* **39**, 103475 (2023).
17. Lu, J. et al. Consistent abnormalities in metabolic patterns of Lewy body dementias. *Mov. Disord.* **37**, 1861–1871 (2022).
18. Meles, S. K. et al. The metabolic pattern of idiopathic REM sleep behavior disorder reflects early-stage Parkinson disease. *J. Nucl. Med.* **59**, 1437–1444 (2018).
19. Holtbernd, F. et al. Dopaminergic correlates of metabolic network activity in Parkinson's disease. *Hum. Brain Mapp.* **36**, 3575–3585 (2015).
20. Shin, J. H. et al. Parkinson disease-related brain metabolic patterns and neurodegeneration in isolated REM sleep behavior disorder. *Neurology* **97**, e378–e388 (2021).
21. Fortin, J.-P. et al. Harmonization of multi-site diffusion tensor imaging data. *Neuroimage* **161**, 149–170 (2017).
22. Fortin, J.-P. et al. Harmonization of cortical thickness measurements across scanners and sites. *Neuroimage* **167**, 104–120 (2018).
23. Arnaldi, D. et al. Presynaptic dopaminergic imaging characterizes patients with REM sleep behavior disorder due to synucleinopathy. *Ann. Neurol.* **95**, 178–1192 (2024).
24. Höglinger, G. U. et al. A biological classification of Parkinson's disease: the SynNeurGe research diagnostic criteria. *Lancet. Neurol.* **23**, 191–204 (2024).
25. Gagnon, J., Postuma, R. B., Joncas, S., Desjardins, C. & Latreille, V. The Montreal Cognitive Assessment: a screening tool for mild cognitive impairment in REM sleep behavior disorder. *Mov. Disord.* **25**, 936–940 (2010).
26. Šubert, M. et al. Spoken language alterations can predict phenoconversion in isolated REM sleep behavior disorder: a multicentric study. *Ann. Neurol.* **95**, 530–543 (2023).
27. Schindlbeck, K. A. et al. Metabolic network abnormalities in drug-naïve Parkinson's disease. *Mov. Disord.* **35**, 587–594 (2020).
28. Orso, B. et al. Validation of the REM behaviour disorder phenoconversion-related pattern in an independent cohort. *Neurol. Sci.* **44**, 3161–3168 (2023).
29. Postuma, R. B. et al. MDS clinical diagnostic criteria for Parkinson's disease. *Mov. Disord.* **30**, 1591–1601 (2015).
30. McKeith, I. G. et al. Diagnosis and management of dementia with Lewy bodies: fourth consensus report of the DLB Consortium. *Neurology* **89**, 88–100 (2017).
31. Berry, R. B. et al. AASM scoring manual updates for 2017 (version 2.4). *J. Clin. Sleep Med.* **13**, 665–666 (2017).
32. Mattioli, P. et al. Cuneus/precuneus as a central hub for brain functional connectivity of mild cognitive impairment in idiopathic REM sleep behavior patients. *Eur. J. Nucl. Med. Mol. Imaging.* <https://doi.org/10.1007/s00259-021-05205-6> (2021).
33. Yoon, E. J. et al. Brain metabolism related to mild cognitive impairment and phenoconversion in patients with isolated REM sleep behavior disorder. *Neurology* **98**, e2413–e2424 (2022).
34. Wahlund, L.-O. et al. A new rating scale for age-related white matter changes applicable to MRI and CT. *Stroke* **32**, 1318–1322 (2001).
35. Litvan, I. et al. Diagnostic criteria for mild cognitive impairment in Parkinson's disease: Movement Disorder Society Task Force guidelines. *Mov. Disord.* **27**, 349–356 (2012).
36. Ahn, H.-J. et al. Seoul Neuropsychological Screening Battery-dementia version (SNSB-D): a useful tool for assessing and monitoring cognitive impairments in dementia patients. *J. Korean Med. Sci.* **25**, 1071–1076 (2010).
37. Gilman, S. et al. Second consensus statement on the diagnosis of multiple system atrophy. *Neurology* **71**, 670–676 (2008).
38. Varrone, A. et al. EANM procedure guidelines for PET brain imaging using [18 F] FDG, version 2. *Eur. J. Nucl. Med. Mol. Imaging* **36**, 2103 (2009).
39. Guedj, E. et al. EANM procedure guidelines for brain PET imaging using [18 F] FDG, version 3. *Eur. J. Nucl. Med. Mol. Imaging* **1–20** (2022).
40. Iber, C. *The AASM Manual for the Scoring of Sleep and Associated Events: Rules, Terminology and Technical Specifications.* Westchester: American Academy of Sleep Medicine (2007).
41. Chang, Y. et al. A new metabolic network correlated with olfactory and executive dysfunctions in idiopathic rapid eye movement sleep behavior disorder. *J. Clin. Neurol.* **15**, 175–183 (2019).
42. Spetsieris, P. G. et al. Metabolic resting-state brain networks in health and disease. *Proc. Natl. Acad. Sci. USA* **112**, 2563–2568 (2015).
43. Meles, S. K., Teune, L. K., de Jong, B. M., Dierckx, R. A. & Leenders, K. L. Metabolic imaging in Parkinson disease. *J. Nucl. Med.* **58**, 23–28 (2017).
44. Meles, S. K. et al. The cerebral metabolic topography of spinocerebellar ataxia type 3. *NeuroImage Clin.* **19**, 90–97 (2018).
45. Fluss, R., Faraggi, D. & Reiser, B. Estimation of the Youden Index and its associated cutoff point. *Biom. J.* **47**, 458–472 (2005).

Acknowledgements

This work was developed within the framework of the DINOGMI Department of Excellence of MIUR 2018–2022 (legge 232 del 2016). The study was partly supported by a grant from the Italian Ministry of Health to IRCCS Ospedale Policlinico San Martino (Fondi per la Ricerca Corrente [to MP], 5 × 1000 founding scheme [to DA], and PNRR POC [to SM]); Funded by the European Union - Next Generation EU - NRRP M6C2 - Investment 2.1 Enhancement and strengthening of biomedical research in the NHS, by the Ministry of University and Research (MUR), National Recovery and Resilience Plan (NRRP), project MNESYS (PE0000006) – A Multiscale integrated approach to the study of the nervous system in health and disease (DN. 1553 11.10.2022) [to MP and CL]; by the Ministry of University and Research (MUR) - PRIN 2022, Protocol N. 20228XKKCM_001 [to CL]. The views and opinions expressed are those of the authors alone and do not necessarily reflect those of the European Union or the European Commission. Neither the European Union nor the European Commission can be held responsible for them. The entire Korean cohort and PET data were supported by a National Research Foundation (NRF) grant funded by the Ministry of Science and ICT (MSIT) in Korea (NRF-2022R1A2C4001834).

Author contributions

(1) Research project: A. Conception, B. Organization, C. Execution; (2) Statistical Analysis: A. Design, B. Execution, C. Review and Critique; (3) Manuscript Preparation: A. Writing of the First Draft, B. Review and Critique. B.O.: 1A, 1B, 1C, 2A, 2B, 3A. P.M.: 1A, 1B, 1C, 2A, 2B. E.J.Y.: 1C, 2C, 3B. Y.K.K.: 1C, 2C, 3B. H.K.: 1C, 2C, 3B. J.H.S.: 1C, 2C, 3B. R.K.: 1C, 2C, 3B. F.F.: 2C, 3B. A.D.: 2C, 3B. F.M.: 1C, 2C, 3B. A.C.: 2C, 3B. M.F.: 2C, 3B. M.S.: 2C, 3B. F.P.: 2C, 3B. M.P.: 1C, 2C, 3B. M.B.: 1C, 2C, 3B. S.M.: 1C, 2C, 3B. J.Y.L.: 1B, 1C, 2C, 3B. C.L.: 1C, 2C, 3B. D.A.: 1A, 1B, 1C, 2A, 2B, 2C, 3A, 3B.

Competing interests

B.O.: received research support from G.E. Healthcare. F.M.: received a speaker honorarium from Roche Diagnostics. M.P.: received research support from Novartis and Nutricia, received fees from Novartis, Merck, and

Biogen. S.M.: speaker Honoraria from G.E. Healthcare, Life Molecular Imaging, and Ely Lilly. D.A.: received fees from Fidia, Jazz, Idorsia, Bruno, Bioprojet, and Lundbeck for lectures, consultation, and board participation. C.L.: no conflict of interest related to the present work. All other authors report no conflicts of interest.

Additional information

Supplementary information The online version contains supplementary material available at <https://doi.org/10.1038/s41531-024-00813-z>.

Correspondence and requests for materials should be addressed to Beatrice Orso.

Reprints and permissions information is available at <http://www.nature.com/reprints>

Publisher's note Springer Nature remains neutral with regard to jurisdictional claims in published maps and institutional affiliations.

Open Access This article is licensed under a Creative Commons Attribution-NonCommercial-NoDerivatives 4.0 International License, which permits any non-commercial use, sharing, distribution and reproduction in any medium or format, as long as you give appropriate credit to the original author(s) and the source, provide a link to the Creative Commons licence, and indicate if you modified the licensed material. You do not have permission under this licence to share adapted material derived from this article or parts of it. The images or other third party material in this article are included in the article's Creative Commons licence, unless indicated otherwise in a credit line to the material. If material is not included in the article's Creative Commons licence and your intended use is not permitted by statutory regulation or exceeds the permitted use, you will need to obtain permission directly from the copyright holder. To view a copy of this licence, visit <http://creativecommons.org/licenses/by-nc-nd/4.0/>.

© The Author(s) 2024